Food Chemistry 524 (2026) 150244

Contents lists available at ScienceDirect

Food Chemistry

journal homepage: www.elsevier.com/locate/foodchem

Enhanced bioaccessibility of pentacyclic triterpenes via interfacial engineering in W/O emulsions

Shiqi Liu [a,b], Yuhui Wang [a], Xinyu Wang [a], Qianqian Li [a], Lulu Zhang [a], Chao Ma [a,*]

[a] College of Biological Science and Technology, Beijing Key Laboratory of Forest Food Processing and Safety, Beijing Forestry University, Beijing 100083, China
[b] Department of Nutrition and Health, China Agricultural University, Beijing 100193, China

ARTICLE INFO

Keywords:
Pentacyclic triterpene
Self-assembly
Interfacial absorption
Water-in-oil emulsions
Bioaccessibility

ABSTRACT

The limited bioaccessibility of pentacyclic triterpenes remains a critical challenge in their practical application. To address this, our study developed novel self-constructed Pickering emulsions by self-assembled pentacyclic triterpene nanoparticles. FTIR analysis confirmed that pentacyclic triterpenes, including ursolic acid (UA), maslinic acid (MA), and betulinic acid (BA), self-assembled into nanoparticles within the oil phase driven by hydrogen bonding between their inherent hydroxy- and carboxyl- groups. Interfacial characterization demonstrated that these self-assembled nanoparticles absorbed onto the water/oil interface to stabilize emulsions. Quantitative analysis revealed distinct interfacial behaviors with MA nanoparticles exhibited the highest interfacial absorption capacity (>95.0%), and the lowest equilibrium interfacial tension (20.6 mN/m), followed by UA and BA nanoparticles. Crucially, *in vitro* simulated gastrointestinal digestion showed that interfacial delivered pentacyclic triterpenes in the resulting emulsions enhanced their bioaccessibility by over 20.0% compared to their free forms. Collectively, this work proposed interfacial engineering via pentacyclic triterpene self-assembly as a promising approach for improving their bioaccessibility.

1. Introduction

Pentacyclic triterpenes are one of the most important natural products (Li et al., 2023), available in a wide range of plant sources, such as vegetables, fruits, cereals, officinal plants, and so on (Hierro et al., 2018; Sohag et al., 2022). Ever-emerging evidence has proved that they are practically non-toxic compounds with various beneficial properties, including but not limited to anticancer (Tang et al., 2022), antiviral (Si et al., 2018), antioxidant (Wang et al., 2010), anti-inflammatory (Zhou et al., 2017), and hepatoprotective effects (Liu et al., 2008). In view of these bioactivities, certain pentacyclic triterpenes have been introduced as functional ingredients in dietary supplements and pharmaceuticals. However, their efficacy is limited by relatively low bioaccessibility. As reported, the bioaccessibility of free oleanolic acid (OA), ursolic acid (UA), and betulin was merely 6.22% (Pan et al., 2025), 0.34% (Liu et al., 2023), and 0.20% (Zeng et al., 2024), respectively.

To overcome this limitation, many delivery vehicles, including liposomes, nanoparticles, and emulsions, have been developed. For example, phospholipid liposomes increased the bioaccessibility of OA by 3.55-time, with further improvements (5.91- and 7.36-time) achieved through chitosan and polygalacturonic acid coatings (Pan et al., 2025). Similarly, gelatin nanoparticles improved the bioaccessibility of UA by 8.46-fold (Karimi et al., 2020), and a self-nanoemulsifying system enhanced the bioaccessibility of 11-keto-β-boswellic acid and acetyl-11-keto-β-boswellic acid by 2.75- and 2.29-fold, respectively (Ting et al., 2018). Despite these advances, safety concerns persist due to the potential toxicity of introduced wall materials, organic solvents, and surfactants, which may cause allergies or intestinal damage (Dai et al., 2015). Therefore, developing novel alternative strategies to enhance the bioaccessibility of pentacyclic triterpene remains critically important. In this context, carrier-free vehicles, leveraging the intrinsic self-assembly behavior of bioactive compounds, emerge as a promising solution to these challenges by eliminating reliance on exogenous carrier materials (Karaosmanoglu et al., 2021).

Pentacyclic triterpenes, comprised of six isoprene units, featured a core skeleton of closed pentacyclic rings with multiple sites available for substitution. Based on their core skeleton structures, they are mainly classified as oleanane-, ursane-, lupane-, and friedelane-type, of which the first three are more common (Montesano et al., 2018). Their unique structures endow their ability to self-assemble. Recently, our team denoted the self-assembly behavior of OA in the oil, facilitating its anchoring at the oil-water interface, further leading to the formation and

* Corresponding author.
E-mail address: machao@bjfu.edu.cn (C. Ma).

https://doi.org/10.1016/j.foodchem.2026.150244
Received 5 January 2026; Received in revised form 15 June 2026; Accepted 28 June 2026
Available online 29 June 2026

stabilization of surfactant-free emulsions (Liu et al., 2024). Importantly, research has proved that these emulsions could improve the bioaccessibility of OA to more than 10.0% (Li et al., 2024), confirming interfacial delivery was an effective approach to improve the bioaccessibility of bioactive ingredients. Inspired by these findings, we reasonably speculate that self-stabilized pentacyclic triterpene emulsions are novel delivery systems to improve their bioaccessibility, with the inherent self-assembly behavior of pentacyclic triterpenes providing the fundamental basis for constructing such systems.

Herein, this study aims to unveil the self-assembly and interfacial absorption behaviors of pentacyclic triterpenes, and to investigate the possibility of the resulting self-stabilized emulsions improving their bioaccessibility. On this basis, three representative pentacyclic triterpenes, including oleanane-type maslinic acid (MA), ursane-type UA, and lupane-type betulinic acid (BA), were chosen to prepare self-constructed emulsions using an ultrasonic emulsification method. The self-assembly mechanism of pentacyclic triterpenes in the oil was elucidated using Fourier transform infrared spectroscopy (FTIR). And the interfacial absorption behaviors of self-assembled nanostructures were analyzed by interfacial wettability, and dynamic interfacial tension. Besides, the gastrointestinal digestion behavior of the formed self-constructed emulsions, and the bioaccessibility of pentacyclic triterpenes within them were assessed. We hypothesized that these pentacyclic triterpenes can self-assemble into interfacially active nanostructures in the oil, enabling the formation of self-stabilized emulsions that enhance the bioaccessibility of them through interfacial delivery.

2. Materials and methods

2.1. Materials

UA, MA, and BA with purity >98% were supplied by Spring & Autumn Biological Engineering (Nanjing, China). Soybean oil was bought from a local store (Beijing, China). HPLC grade phosphoric acid was procured from Shanghai Macklin Biochemical Co., Ltd. (Shanghai, China). HPLC grade acetonitrile, and ethanol were secured from Thermo Fisher Scientific (Waltham, MA, USA). Nile Red, Nile Blue A, pepsin, trypsin, lipase, and bile salt were obtained from Coolaber Science & Technology Co., Ltd. (Beijing, China). Sodium chloride and sodium hydroxide were purchased from Sinopharm Chemical Reagent Co., Ltd. (Shanghai, China). Concentrated hydrochloric acid was bought from Modern Oriental (Beijing) Technology Development Co., Ltd. (Beijing, China). Water was generated using a Synergy 185 Ultrapure Water System (Millipore, MA, USA).

2.2. Self-stabilized emulsions preparation

Pentacyclic triterpene-based emulsions were fabricated using an ultrasonic-assisted emulsification method. Briefly, a certain amount of each pentacyclic triterpene (UA, MA, BA) was added to the oil (1.0%, *w/v*), and then completely dispersed by ultrasonication for 20 s (20 kHz, Cole-Parmer, Vernon Hills, IL, USA). Then, water was added to the resulting oil phase with a final water phase volume fraction of 0.4 (*v/v*), followed by ultrasonic treatment for another 30 s to obtain emulsions.

2.3. Microstructure observation

The microstructures of emulsions were observed using optical microscope, CLSM, and cryo-SEM. For optical microscope observation, a drop of freshly prepared emulsions was put on a glass slide, and then covered with a cover slip for 630 × magnification observation. Then, the images were captured with a DMi8 inverted microscope instrument (Leica, Frankfurt, Germany) equipped with a DFC 9000 microscope camera, and the droplet size of emulsions was measured by Image J software (National Institutes of Health, Bethesda, MD, USA). For CLSM observation, Nile red (0.01%, *w/v*) and Nile blue A (0.1%, *w/v*) were added to oil and water for pre-staining before emulsification, respectively. Then, the stained sample was spread on a glass slide, and covered with a cover slip for observation under a 63 × oil immersion lens. The images were captured with a CLSM instrument (SP8, Leica, Frankfurt, Germany) at excitation wavelengths of 488 nm and 633 nm. For cryo-SEM observation, a drop of emulsions was dropped onto a copper specimen holder and immediately frozen in liquid nitrogen, followed by transfer to the cryo-preparation chamber by a transmission system (PP3010T, Quorum, UK) for sample fracture. Subsequently, the sample was sublimated at −90 °C for 5 min, and then coated with sputtered gold particles (10 mA, 60 s). Afterward, the sample was inserted into the observation chamber, and the images were taken using a Helios Nano-Lab G3 UC scanning electron microscope (SEM, FEI, MA, USA) at an accelerating voltage of 2 kV.

The morphologies of pentacyclic triterpenes were visualized using an SEM instrument (Regulus 8100, Hitachi, Tokyo, Japan). Briefly, each pentacyclic triterpene was fixed on the aluminum pan, and then gold-plated by a sputter coater (MC 1000, Hitachi, Tokyo, Japan). After which, their morphologies were observed under an accelerating voltage of 10 kV.

2.4. Fourier transform infrared spectroscopy (FTIR) determination

The molecular interactions between pentacyclic triterpenes were studied using FTIR. Briefly, each pentacyclic triterpene was combined with potassium bromide (KBr), after which they were compressed into tablets for FTIR scanning. Each mixture of pentacyclic triterpene and oil after ultrasonication was directly spread onto a transparent KBr tablet for FTIR scanning. Then, their infrared spectra were recorded in the region of 4000–500 cm^{-1} with a resolution of 4 cm^{-1} (Nicolet IS 5, Thermo Fisher Scientific, Waltham, MA, USA).

2.5. Wettability measurement

The three-phase contact angle of each pentacyclic triterpene nanoparticle was measured using a sessile drop method for wettability analysis. In brief, each pentacyclic triterpene nanoparticle was compressed into a tablet at 20 MPa (YP-15, Tianjin Hench Technology Co., Ltd., Tianjin, China), after which it was placed into the bottom of a glass cuvette containing oil. Then, a water droplet was injected onto the tablet surface, and the shape of the droplet was automatically recorded by an OCA20 contact angle measuring device equipped with a high-speed camera (Dataphyscis, Berlin, Germany). And the corresponding three-phase contact angle was then calculated using the Young equation.

2.6. Interfacial behavior analysis

The interfacial absorption kinetics of each pentacyclic triterpene nanoparticle were analyzed using a pendant drop method. Briefly, oil containing pentacyclic triterpene nanoparticles was placed into the syringe, and immersed into a transparent glass cuvette filled with water. Then, oil was slowly injected into the water until a pendant droplet was formed, after which standing for 3600 s at ambient temperature to ensure the absorption of pentacyclic triterpene nanoparticles at the oil-water interface. The formed droplet shape was constantly recorded using an LSA 100 optical contact angle meter, and the interfacial tension was calculated based on the Young equation (LAUDA Scientific, Lauda, Germany). Then, the surface pressure (π) was calculated using the following equation.

$$\pi\ (\mathrm{mN/m}) = \gamma_0 - \gamma$$

where γ_0 and γ are the interfacial tensions between water and free oil/oil containing pentacyclic triterpene nanoparticles, respectively.

And the change in π versus time can be expressed by the modified

form of the Ward and Tordai equation (Qin et al., 2022).

$$\pi\ (mN/m) = 2C_0K_BT(D_t/3.14)^{1/2}$$

where C_0 is the concentration of continuous phase, K_B is the Boltzmann constant, T is the absolute temperature, and D_t is the diffusion coefficient at t time.

Further, the interfacial penetration and reorganization of pentacyclic triterpene nanoparticles were explored according to the first-order equation.

$$\ln\ (\pi_{3600}\text{-}\pi_t)\ /(\pi_{3600}\text{-}\pi_0) = -kt$$

where π_0, π_{3600}, and π_t are the surface pressure at the beginning, final, and t time, respectively, k is the first-order rate constant, and t is the absorption time.

The interfacial absorption capacity was determined according to (Fan et al., 2023) with a slight modification. Briefly, freshly prepared emulsions were centrifuged at 10,000 ×*g* at 4 °C for 30 min, after which the leaked oil layer was collected. Afterward, the concentrations of pentacyclic triterpenes in the initial emulsions and collected oil layer were determined using an HPLC method. Namely, ethanol was added to the sample, followed by *v*igorous vortexing to fully dissolve the sample, and then filtered using a 0.22 μm filter for further HPLC analysis (LC-20AT, Shimadzu, Kyoto, Japan). The separation of pentacyclic triterpenes was conducted at 30 °C on a Diamonsil C18 column (250 mm × 4.6 mm; Dikma Co. Beijing, China). Acetonitrile and 0.1% phosphoric acid aqueous solution were used as the mobile phases (95:5, *v/v*), and the flow rate was set at 1.0 mL/min with an injection volume of 5 μL. Then, the chromatogram of each pentacyclic triterpene was recorded at 205 nm, and their concentrations were calculated based on the standard curves of 5–500 μg/mL ($r = 1$). Finally, the interfacial absorption capacity of each pentacyclic triterpene was calculated as follows.

$$\text{Interfacial absorption capacity (\%)} = (C_0 \times V_0\text{-}C_1 \times V_1)/(C_0 \times V_0) \times 100\%$$

where C_0 and C_1 are pentacyclic triterpene concentrations in the freshly prepared emulsions and collected oil layer, respectively. V_0 and V_1 are the volumes of freshly prepared emulsions and collected oil layer, respectively.

2.7. Rheological characterization

The rheological behaviors of emulsions were characterized using an MCR 302e rheometer (Anton Paar, Graz, Austria) equipped with a cylinder (diameter of 28.902 mm), and the gap was set to 5.0 mm. Strain sweep was conducted from 0.01% to 100% at a fixed frequency of 1 Hz to determine the linear viscoelastic region (LVR), within which the following angular frequency sweep was conducted. Angular frequency sweep was performed in the range of 0.1–100 rad/s at a fixed strain of 0.1%. Apparent viscosity sweep was carried out with the shear rate increasing from 0.01 to 100 s^{-1}.

2.8. Gastrointestinal digestive behavior analysis

The digestion behavior of pentacyclic triterpene-structured emulsions in the simulated gastrointestinal fluids was evaluated as follows. Firstly, the simulated gastric fluids (SGF) and simulated intestinal fluids (SIF) were formulated according to our established protocol (Liu et al., 2024). Then, each sample was separately added to the SGF for 2 h of digestion, followed by transfer to the SIF for another 4 h of continuous digestion. After the SIF digestion, the digestive fluids were collected and centrifuged at 12,000 ×*g* for 30 min at 4 °C. The obtained micellar phase was then separated and absolute ethanol was added to fully extract pentacyclic triterpenes, which was then subjected to further HPLC analysis. And the bioaccessibility of pentacyclic triterpenes was calculated as follows.

$$\text{Bioaccessibility (\%)} = m_1/m_0 \times 100\%$$

where m_0 and m_1 are the content (mg) of pentacyclic triterpene in the initially added and digestive micelles, respectively.

During intestinal digestion, the free fatty acid (FFA) released from the hydrolysis of oil by lipase was recorded by the pH-stat method with slight modifications (Zhou et al., 2023). Briefly, the pH of the digest was kept constant at 7.0 by titrating 0.1 mol/L NaOH at certain time intervals, and the percentage of FFA released was calculated by the consumed NaOH volume using the following formula.

$$\text{FFA (\%)} = C_{NaOH} \times V_{NaOH} \times M_{oil}/2m_{oil}.$$

where C_{NaOH} represents the concentration (mol/L) of NaOH used for titration, V_{NaOH} is the consumed NaOH volume (mL), M_{oil} means the average molecular weight (g/moL) of soybean oil, and m_{oil} is the mass (g) of oil in the initially added emulsions.

After each digestive stage, the particle size and zeta potential of the digests were measured based on a published method with slight modifications (Li et al., 2024). Briefly, the particle size was determined using a Mastersizer 3000 analyzer (Malvern, Great Malvern, UK). The stirring speed was set to 2000 rpm, and the obscuration was set between 10% and 20%. The refractive indices of soybean oil and water were 1.476 and 1.33, respectively. Besides, the zeta potential was tested using a Zetasizer Nano ZS90 instrument (Malvern, Great Malvern, UK). After the intestinal digestive stage, the microstructure of the digests was observed using a CLSM instrument. Oil droplets were stained with Nile red (0.01%, *w/v*), with an excitation wavelength set to 488 nm, and the images were captured under a 10 × objective lens.

2.9. Statistical analysis

All experiments were conducted in triplicate with results expressed as mean values ± standard deviation (SD). Data were statistically analyzed by one-way analysis of variance (ANOVA) with multiple comparisons made using Duncan's test (SPSS 19.0, SPSS Inc., Chicago, USA), and $P < 0.05$ was considered statistically significant. The presented results were plotted using Origin 2018 software (Origin Lab Corp., Northampton, USA).

3. Results and discussion

3.1. Preparation of self-stabilized emulsions

Herein, emulsions were constructed by ultrasonic emulsification method at a fixed pentacyclic triterpene concentration of 1.0% (*w/v*). As seen in Fig. 1A, visual appearances of all the samples exhibited similar creamy and homogeneous textures, suggesting the successful formation of emulsions in the presence of UA, MA, and BA. In other words, UA, MA, and BA had good emulsifying ability to stabilize emulsions. Microscopic observations also showed that many micron-sized spherical emulsion droplets were distributed in each emulsion (Fig. 1B), however, their droplet sizes were significantly different (Fig. 1C). Statistically, the smallest average droplet size of 3.42 μm was observed in UA emulsions, followed by MA emulsions (5.11 μm) and BA emulsions (10.56 μm). To further determine the emulsion type, oil and water were dyed with Nile red and Nile blue A, which appeared green and red in CLSM images, respectively. It was clearly visible that in all emulsions, the red emulsion droplets were dispersed in the green continuous phase (Fig. 1D), confirming that they were all W/O type.

3.2. Stabilization mechanism of self-stabilized emulsions

3.2.1. Microscopic observation

In order to reveal the stabilization mechanism of emulsions and directly observe the distribution of pentacyclic triterpene, the internal

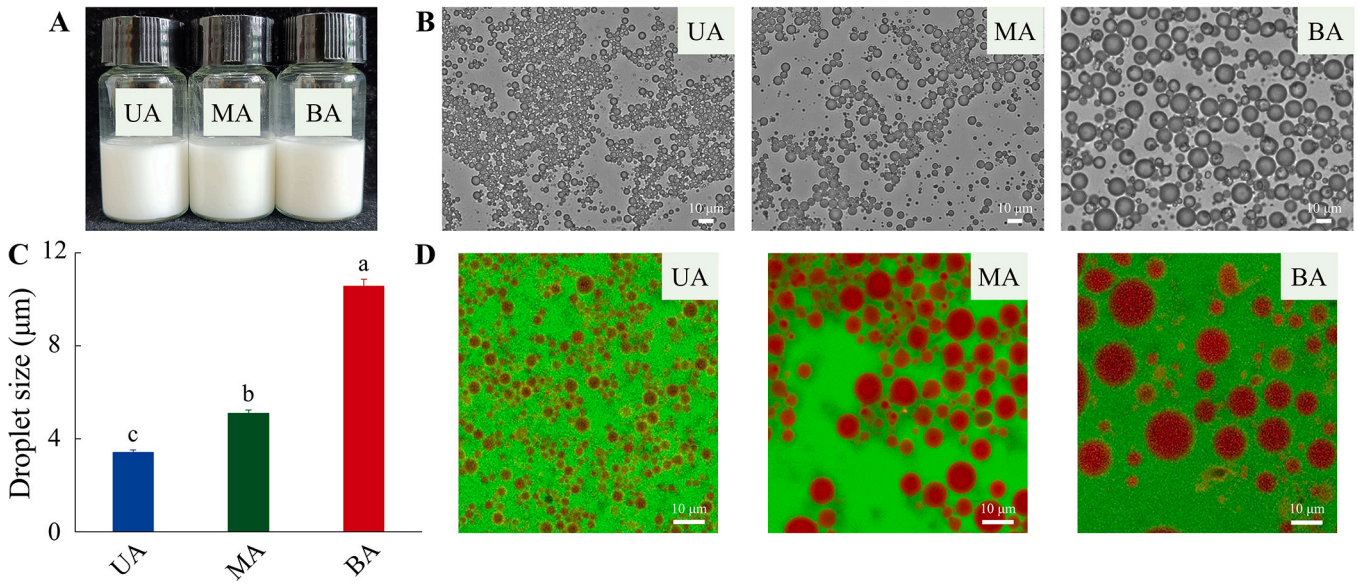

Fig. 1. Appearances (A), optical images (B), droplet size (C), and CLSM images (D) of pentacyclic triterpene-structured emulsions. UA, ursolic acid; MA, maslinic acid; BA, betulinic acid. Data were presented as mean values ± standard deviation (SD) from three independent experiments ($n = 3$). Different letters indicate significant differences among treatments ($P < 0.05$).

microstructures were characterized in more depth using cryo-SEM. As observed in Fig. 2A, many spherical water droplets and indentations were visible in the cross-section, which was identical to the optical microscopy observation. When zooming in one water droplet, the surface was clearly covered with abundant and interconnected nano-sized structures. These nanostructures formed a dense interfacial film, leading to the stabilization of emulsions (Gu et al., 2022). Notably, the shape of nanostructures varied in different emulsions. Among them, nanospheres appeared in UA and MA emulsions, while nanofibers were present in BA emulsions. Nevertheless, crude UA and BA presented rod-like structures with micrometer-scale lengths, and MA showed micron-sized sheet-like structures (Fig. 2B), all of which were totally different from the nanostructures seen above. According to previous work (Bag & Majumdar, 2017; S. Liu, Liu, Li et al., 2024), pentacyclic triterpenes such as UA, MA and BA have a rigid backbone that can maintain nano-forms in solutions, and the presence of hydrogen bonded donors and receptors in their structures (Fig. 3A-3C) contributes to form hydrogen bonds, thereby enabling them to spontaneously form supramolecular architectures in response to high temperature or ultrasonication. Thus, we speculated that these nanostructures were the result of their self-assembly.

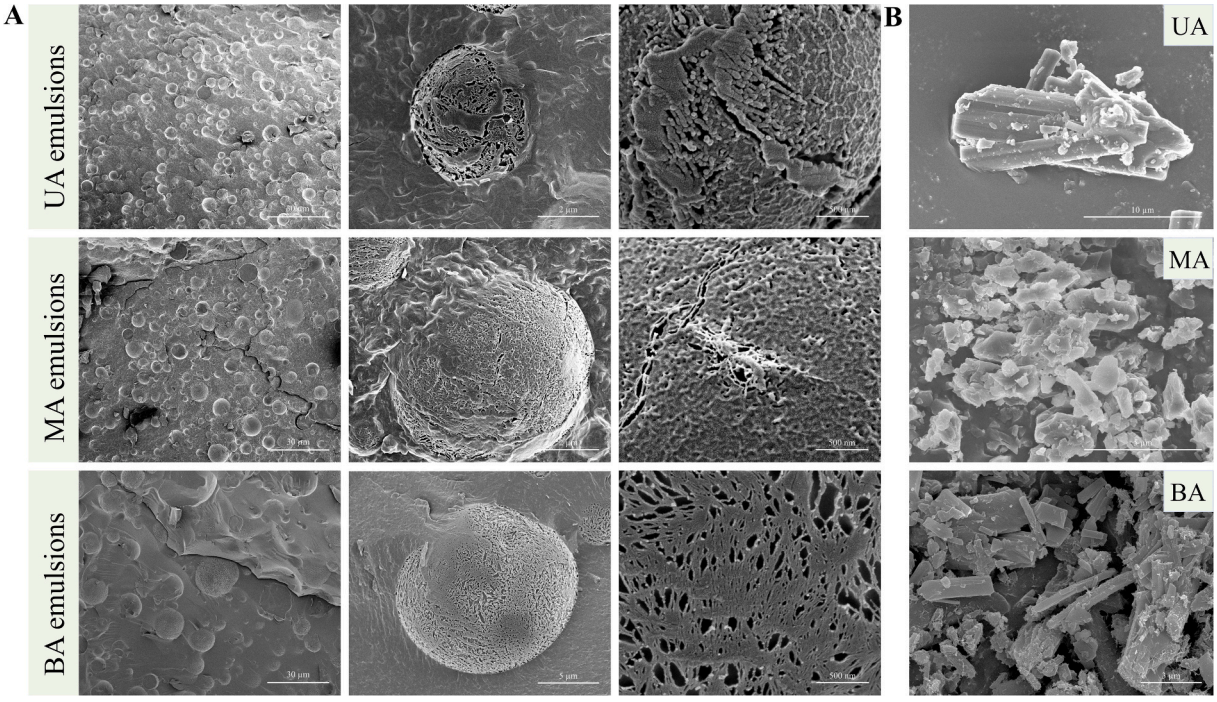

Fig. 2. Cryo-SEM images of pentacyclic triterpene-structured emulsions (A); SEM images of free pentacyclic triterpenes (B). UA, ursolic acid; MA, maslinic acid; BA, betulinic acid.

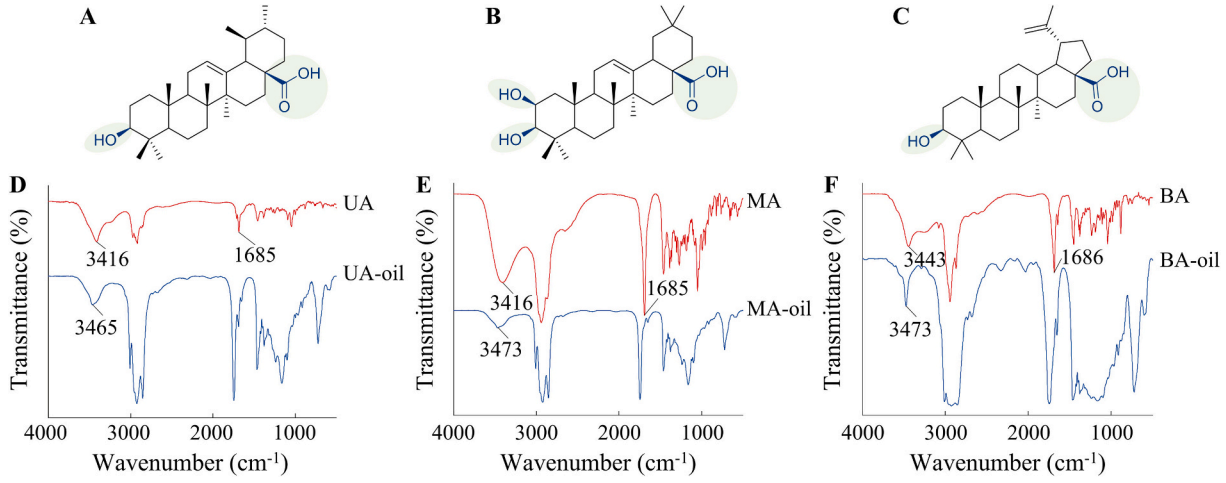

Fig. 3. Molecular structures of free pentacyclic triterpenes. UA (A); MA (B); BA (C). FTIR spectra of pentacyclic triterpenes/pentacyclic triterpene nanoparticles in the oil. UA (D); MA (E); BA (F). UA, ursolic acid; MA, maslinic acid; BA, betulinic acid.

3.2.2. *FTIR analysis*

To prove our hypothesis, FTIR was conducted to compare the spectral differences of pentacyclic triterpenes before and after ultrasonication. As illustrated in Fig. 3D-3F, the characteristic peaks with respect to hydroxyl (-OH) and carboxyl (-COOH) groups in crude UA, MA, and BA were observed at 3416 and 1685 cm^{-1}, 3416 and 1685 cm^{-1}, and 3443 and 1686 cm^{-1}, respectively (Diego A. Bravo-Alfaro et al., 2022; Mu et al., 2024; J. Wang et al., 2020). After ultrasonication in the oil, the absorption bonds attributed to -OH group shifted to higher wavenumber, while the peaks corresponding to -COOH disappeared. These results indicated the formation of hydrogen bonds between -OH and -COOH groups (Liu et al., 2022), further confirming that the self-assembly of pentacyclic triterpenes occurred during ultrasonication.

As evident from the abovementioned results, the formation and stabilization mechanism of self-structured pentacyclic triterpene emulsions can be concluded as follows. With the aid of ultrasonication, these three pentacyclic triterpenes were self-assembled into nanostructures through hydrogen bonds in the oil. After the addition of water, emulsified droplets were formed due to the cavitation effect (Geng et al., 2023). And these nanostructures were absorbed onto the surface of droplets, forming an interfacial film that avoided direct contact between oil and water, thus leading to the formation and stabilization of Pickering emulsions.

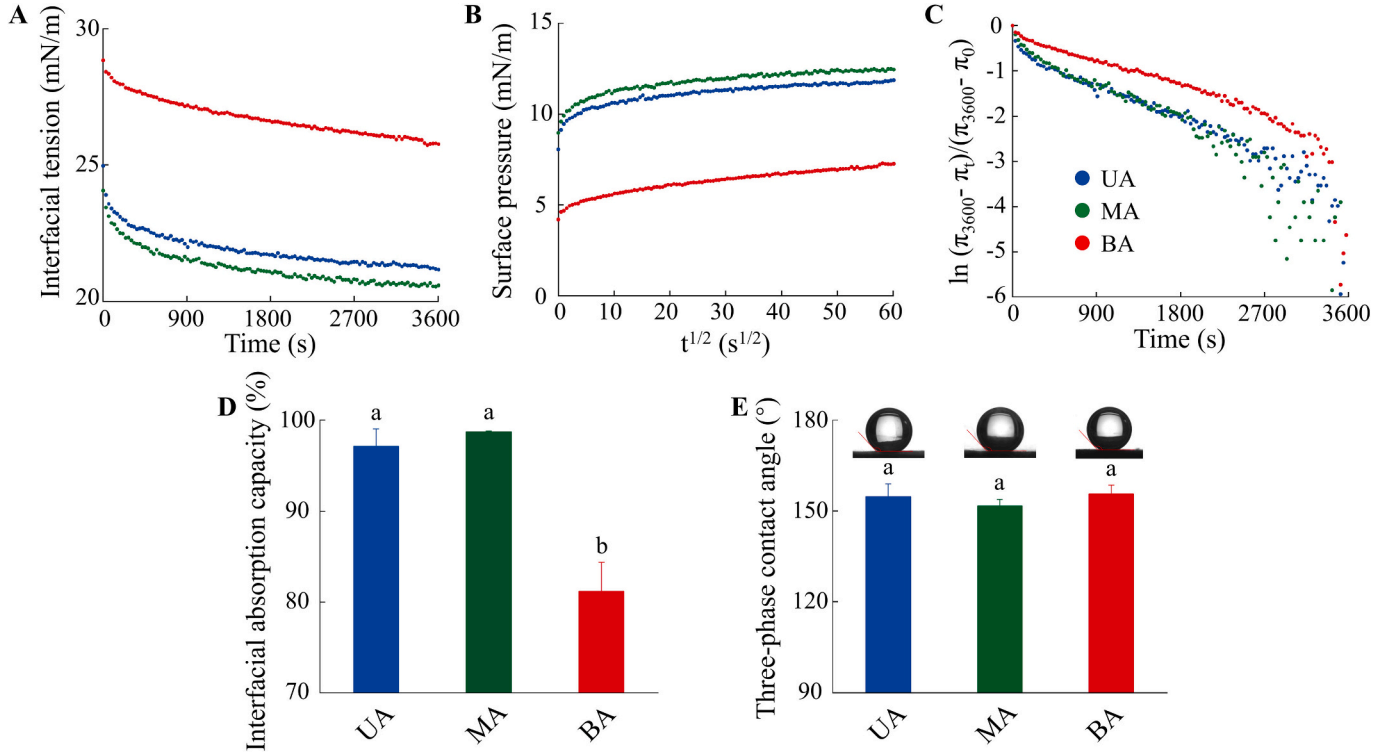

Fig. 4. Interfacial tension (A), surface pressure (B), adsorption kinetics (C), interfacial viscoelasticity (D), absorption capacity (E), and three-phase contact angle (F) of pentacyclic triterpene nanoparticles at the oil-water interface. UA, ursolic acid; MA, maslinic acid; BA, betulinic acid. Data were presented as mean values ± standard deviation (SD) from three independent experiments (n = 3). Different letters indicate significant differences among treatments ($P < 0.05$).

3.3. Interfacial behavior analysis

3.3.1. Dynamic interfacial tension

Afterwards, the adsorption behavior of these nanostructures at the oil-water interface was quantitatively assessed by recording the dynamic interfacial tension between oil containing different pentacyclic triterpene nanoparticles and water (Guo et al., 2024). As illustrated in Fig. 4A, the interfacial tension in all systems displayed a sharp decrease in a short time, and then a gradual decrease to an equilibrium level was observed. This was indicative of the rapid diffusion of nanoparticles from the oil phase to the oil-water interface at the earlier absorption period, followed by a saturation of their interfacial adsorption. A similar phenomenon was also found in the dynamic interfacial tension profile between oil and water containing cyclodextrins (Cheng et al., 2023). Ultimately, the system containing MA nanoparticles had the lowest interfacial tension of 20.6 mN/m, followed closely by UA nanoparticles of 21.2 mN/m and BA nanoparticles of 25.8 mN/m. This noted that MA had the strongest interfacial adsorption ability (Fan et al., 2024). It was also worth noting that the pure oil-water interfacial tension of 33.0 mN/m was determined in our previous study (Lu et al., 2024). Compared with this, the reduction in interfacial tension after adding pentacyclic triterpene nanoparticles was not as much as adding surfactants like PGPR (Gülseren & Corredig, 2014). These results implied that emulsions structured by pentacyclic triterpene were mainly stabilized by steric hindrance rather than lowering the interfacial tension, which was also the typical characteristic of Pickering stabilization (Liu et al., 2022).

According to Cheng et al. (2023), the adsorption process of pentacyclic triterpene nanoparticles onto the oil-water interface involves diffusion, penetration and rearrangement. As exhibited in Fig. 4B, the surface pressure (π) was linearly related to the square root of time ($t^{1/2}$), demonstrating that the absorption of these nanoparticles was predominantly governed by diffusion, and the slope represents the diffusion rate (k_{diff}) (Liang et al., 2024). The calculated K_{diff} was 1.3857, 0.9304, and 0.4850 mN/m/$s^{1/2}$ for MA, UA, and BA nanoparticles, respectively, denoting that MA nanoparticles possessed the strongest diffusion capability and the fastest adsorption rate to form the interfacial film. As stated by Liang et al. (2024), a higher K_{diff} correlates with a lower interfacial tension, which aligns with the abovementioned results. And the permeation and rearrangement processes can be described using a first-order kinetic equation. There were two linear regions in the curve of ln (π_{3600}-π_t) /(π_{3600}-π_0) versus t (Fig. 4C), where the slopes sequentially corresponded to the permeation rate (K_p), and the rearrangement rate (K_R). Among them, the K_p of MA and UA nanoparticles were 0.0008 to 0.0009 s^{-1}, which were higher than that of BA nanoparticles (0.0006 s^{-1}), indicating that MA and UA nanoparticles had similar permeation rates at the interface, both of which were faster than that of BA nanoparticles. Besides, the K_R of UA nanoparticles was the largest (0.0016 s^{-1}), while the K_R of the other two was comparable, ranging from 0.0012 to 0.0013 s^{-1}.

3.3.2. Interfacial absorption capability

The amounts of these nanoparticles absorbed on the interface were determined and summarized in Fig. 4D. BA presented a relatively lower interfacial adsorption capacity of only 81.2%. In comparison, both MA and UA nanoparticles showed high interfacial absorption capacities exceeding 95.0% with no significant difference, suggesting more molecules were anchored on the interface. And this was the fundamental reason for the difference in the interfacial tension (Liang et al., 2024). Finally, the interfacial wettability of these nanoparticles was characterized using the three-phase contact angle. As can be seen in Fig. 4E, all the pentacyclic triterpene nanoparticles exhibited a three-phase contact angle greater than 90°, suggesting they were preferentially wetted by the oil phase, further conducive to forming W/O emulsions. Furthermore, their three-phase contact angles ranged from 151° to 156° with no significant differences, indicating that their wettability was comparable.

3.4. Rheology properties

Rheology properties are effective tools for reflecting the stability of the emulsions (Hei et al., 2024). Herein, strain, frequency and apparent viscosity sweep of pentacyclic triterpene-structured emulsions were carried out to analyze their rheological behaviors. As shown in Fig. 5A, the strain independence of the G′ and G″ values was observed at low shear strains, which was identified as LVR (Wang et al., 2024). In the LVR, the G′ value in the MA and UA emulsions was lower than the G″ value, indicating these emulsions were characterized by viscous properties. Whereas the G′ value in the BA emulsions was greater than the G″ value, which indicated elastic-dominated structures. However, as the shear strain increased, the G′ value gradually decreased, and the G″ value increased until they intersected. This was because the structure of BA emulsions was destroyed, and their solid states transitioned to liquid states (Gu et al., 2023). When the strain was fixed at 0.1%, the G′ value in BA emulsions consistently surpassed the G″ value over the entire frequency range, presenting solid-like structures. For MA and UA emulsions, the G″ value was always higher than the G′ value, exhibiting liquid-like structures (Fig. 5B). Under the shear forces, the apparent viscosity of all samples decreased as the shear rate increased (Fig. 5C), which was typical of non-Newtonian pseudo-plastic fluids (Hei et al., 2024). Within the shear rate range of 0.01–100 s^{-1}, BA emulsions had much higher viscosity than that of UA and MA emulsions, which may be due to its solid-like structure. However, its viscosity decreased drastically when subjected to a higher shear rate, indicating a severe destruction of its structure.

3.5. Gastrointestinal digestive behavior analysis

Low bioaccessibility of pentacyclic triterpenes limits their efficacy for use, which is a critical issue that needs to be solved urgently (Liu, Liu, Zhang, et al., 2024). As evidenced in Fig. 6A, the bioaccessibility of free UA, MA, and BA was merely 2.8%, 1.9%, and 1.7%, respectively. In comparison, when they were employed as Pickering stabilizers to form self-stabilized emulsions, a significant enhancement in their bioaccessibility was observed. Specifically, the bioaccessibility of UA within the emulsions markedly increased by 8.9-fold, while MA and BA exhibited substantial increases of 14.6-fold and 13.1-fold, respectively. This enhancement was attributed to the following process. Lipid hydrolysis was initially catalyzed by bile salts and lipase during digestion, generating FFA that facilitated the formation of mixed micelles (Liu et al., 2023). Concurrently, bile salts competitively absorbed at the oil-water interface, partially displacing the pentacyclic triterpene molecules and squeezed into the continuous phase. The progression insertion of bile salts and FFA into the interfacial film gradually destabilized the emulsions (Yan et al., 2023). The detached pentacyclic triterpenes (UA, MA, and BA) were then solubilized into the hydrophobic cores of mixed micelles formed by bile salts, phospholipids, and FFA, thereby improving their bioaccessibility. This aligns with established literature confirming that lipid phases significantly enhance the bioaccessibility of hydrophobic bioactive compounds, such as carotenoids and polyphenols (Thakur et al., 2020). And the corresponding FFA release results were quantified in Fig. 6B. FFA release kinetics in all samples showed an initial burst within the first 5 min, followed by sustained release over the subsequent 235 min. A similar release profile was also found in self-constructed oleanolic acid emulsions (Li et al., 2025). Crucially, the cumulative FFA release after 240 min of intestinal digestion differed significantly between emulsions. MA emulsions released the highest amount of FFA (61.7%), followed by UA emulsions (54.0%), and BA emulsions (45.5%). This result was conversely proportional to the modulus of emulsions. As expected, higher FFA release favored the generation of mixed micelles that would be available to dissolve pentacyclic triterpenes, further contributing to higher bioaccessibility.

The particle size of the digests from different samples after digestion was illustrated in Fig. 6C. After intestinal digestion, all three systems

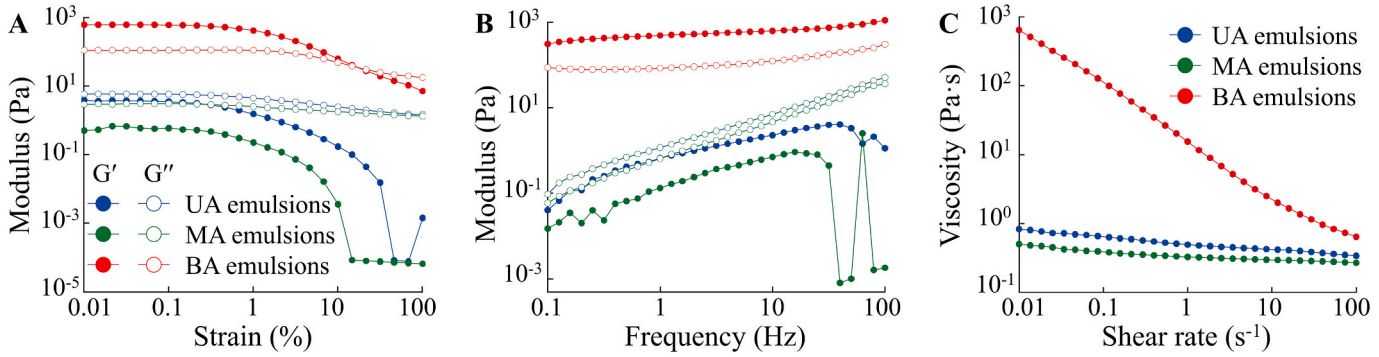

Fig. 5. Rheological behaviors of pentacyclic triterpene-structured emulsions. Amplitude sweep (A); Frequency sweep (B); Flow sweep (C). UA, ursolic acid; MA, maslinic acid; BA, betulinic acid.

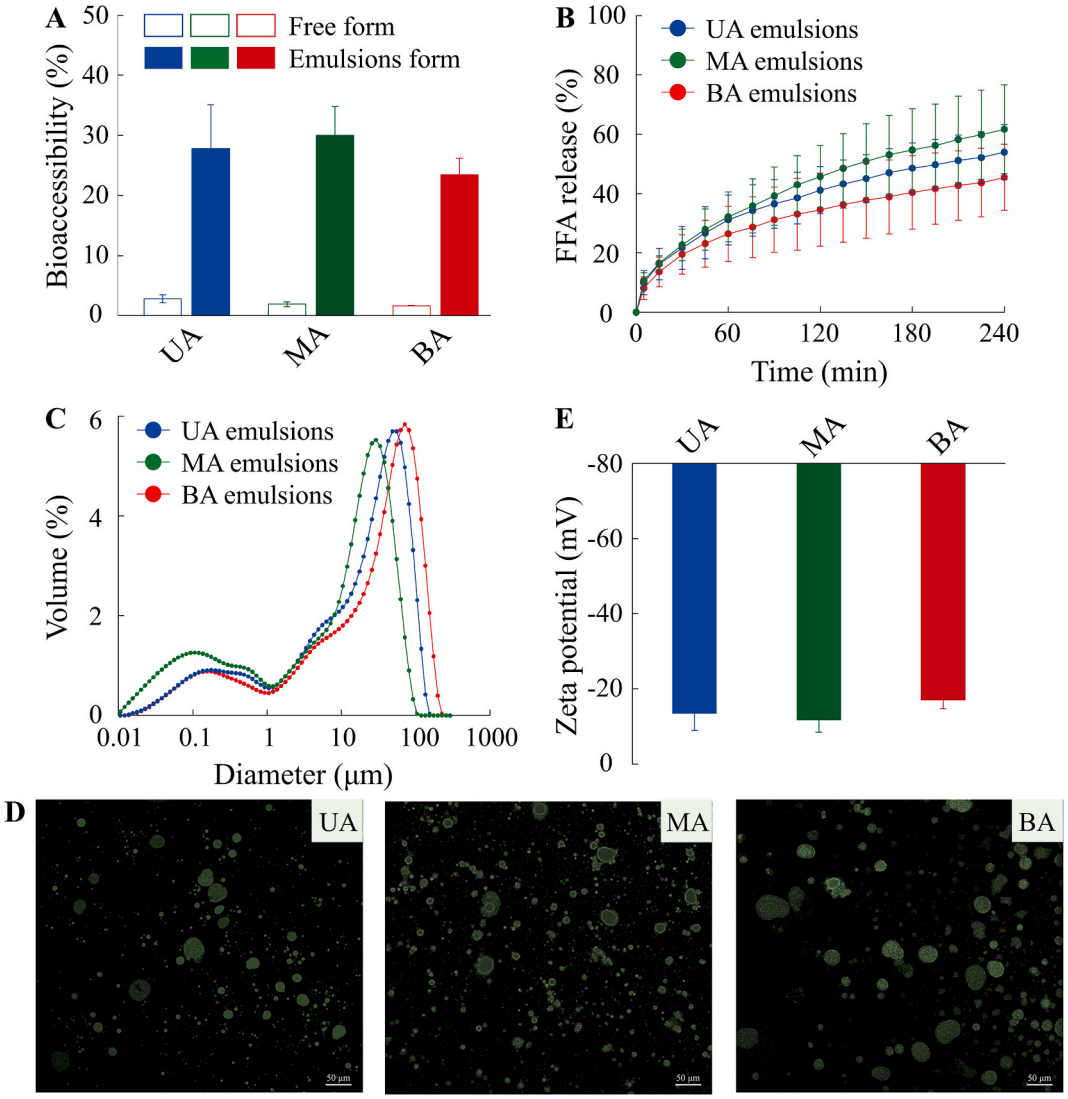

Fig. 6. Bioaccessibility of pentacyclic triterpenes in free and emulsion forms (A); Release profile of free fatty acid (FFA) from pentacyclic triterpene-structured emulsions (B); Particle size (C), CLSM images (D), and zeta potential (E) of pentacyclic triterpene-structured emulsions after *in vitro* simulated digestion. UA, ursolic acid; MA, maslinic acid; BA, betulinic acid. Data were presented as mean values ± standard deviation (SD) from three independent experiments (n = 3). Different letters indicate significant differences among treatments ($P < 0.05$).

presented a bimodal profile (0.01 to 300 μm), characterized by a minor peak near 0.1 μm and a dominant peak at approximately 50 μm. This distribution mainly corresponded to mixed micelles and undigested oil droplets (Li et al., 2024). Notably, digests from MA emulsions displayed the smallest average particle size, followed by UA and BA emulsions. This size hierarchy aligned with the observed FFA release profiles,

wherein greater lipase-mediated hydrolysis of lipids in MA emulsions likely contributed to reduced droplet dimensions. This inference was corroborated by Nile red-stained fluorescence microscopy (Fig. 6D), which visually confirmed the presence of smaller lipid droplets in MA digests compared to UA and BA systems. Furthermore, all samples exhibited strongly negative zeta potentials (Fig. 6E), attributable to surface-adsorbed anionic species (such as FFA and bile salts). Among them, the digests in MA emulsions had the strongest zeta potential, followed by UA emulsions and BA emulsions. The variation in zeta potential among samples may reflect differences in the extent of lipid digestion and the composition of anionic components at the droplet interface (Liu et al., 2023).

4. Conclusion

This study successfully developed self-stabilized W/O Pickering emulsions by the self-assembled nanostructures of pentacyclic triterpenes (UA, MA, and BA) through the ultrasonic emulsification method. FTIR analysis confirmed they self-assembled into nanoparticles driven by hydrogen bonding between hydroxyl- and carboxyl- groups. Cryo-SEM showed that these self-assembled nanostructures adsorbed at the oil-water interface forming dense interfacial films, resulting in emulsion stabilization. Interfacial analysis revealed that MA nanoparticles exhibited the strongest adsorption capacity (98.7%), and the lowest equilibrium interfacial tension (20.6 mN/m), followed by UA nanoparticles (97.2%, 21.2 mN/m) and BA nanoparticles (81.2%, 25.8 mN/m). In contrast, BA emulsions displayed the highest elastic modulus and viscosity, followed by UA emulsions and MA emulsions. Compared with free forms, UA, MA, and BA in the resulting emulsions significantly enhanced bioaccessibility by 25.0%, 28.1%, and 21.8%, respectively. This improvement was attributed to lipid hydrolysis during digestion, with MA emulsions releasing the highest FFA (61.7%), followed by UA emulsions (54.0%) and BA emulsions (45.5%), forming abundant mixed micelles that efficiently solubilized pentacyclic triterpenes. Correspondingly, the digests in MA emulsions showed the smallest particle size and the strongest zeta potential, followed by UA emulsions and BA emulsions. Overall, this work provided insights into the development of self-constructed Pickering emulsions for improving the bioaccessibility of pentacyclic triterpenes.

CRediT authorship contribution statement

Shiqi Liu: Writing – original draft, Investigation, Funding acquisition, Formal analysis, Data curation, Conceptualization. **Yuhui Wang:** Investigation. **Xinyu Wang:** Formal analysis, Data curation. **Qianqian Li:** Formal analysis, Data curation. **Lulu Zhang:** Formal analysis, Data curation. **Chao Ma:** Writing – review & editing, Validation, Funding acquisition, Conceptualization.

Declaration of competing interest

The authors declare that they have no known competing financial interests or personal relationships that could have appeared to influence the work reported in this paper.

Acknowledgements

This work was supported by the National Natural Science Foundation of China (32502079, 31770614), the Postdoctoral Fellowship Program of CPSF (GZC20251960), the Science and Technology Innovation Program of Xiongan New Area (XA2026211308K, 2025XAGG0054), the Fundamental Research Funds for the Central Universities (PTJS202625, QNTD202507) , and the Key Research and Development Program of Xinjiang Uygur Autonomous Region (2025B02007-3).

Data availability

Data will be made available on request.

References

Bag, B. G., & Majumdar, R. (2017). Self-assembly of renewable nano-sized triterpenoids. *The Chemical Record, 17*, 1–34. https://doi.org/10.1002/tcr.201600123

Bravo-Alfaro, D. A., Ochoa-Rodríguez, L. R., Villaseñor-Ortega, F., Luna-Barcenas, G., & García, H. S. (2022). Self-nanoemulsifying drug delivery system (SNEDDS) improves the oral bioavailability of betulinic acid. *Journal of Molecular Liquids, 364*, 119946–119958. https://doi.org/10.55218/jasr.s2202112301

Cheng, C., Yuan, C., Cui, B., Lu, L., Li, J., & Sha, H. (2023). Interfacial behavior of cyclodextrins at the oil-water interface of Pickering emulsion. *Food Hydrocolloids, 134*, 108104–108114. https://doi.org/10.1016/j.foodhyd.2022.108104

Dai, L., Cao, X., Liu, K., Li, C., Zhang, G., Deng, L., Si, C., He, J., & Lei, J. (2015). Self-assembled targeted folate-conjugated eight-arm-polyethylene glycol–betulinic acid nanoparticles for co-delivery of anticancer drugs. *Journal of Materials Chemistry B, 3*, 3754–3766. https://doi.org/10.1039/c5tb00042d

Fan, C., Wang, X., Feng, T., Xia, S., Yu, J., & Swing, C. J. (2023). Tannic acid enhanced the oxidation stability of vitamin A-vitamin D3 coencapsulated in emulsion based on OSA starch/chitosan: Interfacial absorption, antioxidation and viscoelasticity. *Food Hydrocolloids, 144*, 108912–108921. https://doi.org/10.1016/j.foodhyd.2023.108912

Fan, S., Richel, A., Yang, Q., Wang, D., Fauconnier, M.-L., Zhu, C., Yang, W., Wen, X., Hou, C., Li, X., & Zhang, D. (2024). Zein and tannic acid hybrid particles improving physical stability, controlled release properties, and antimicrobial activity of cinnamon essential oil loaded Pickering emulsions. *Food Chemistry, 446*, 138512–138524. https://doi.org/10.1016/j.foodchem.2024.138512

Geng, Z., Zhou, L., Zhang, L., & Hu, J. (2023). Controllable emulsification by dissolved gas in water: Formation and stability of surfactant-free oil nanodroplets. *Colloids and Surfaces A: Physicochemical and Engineering Aspects, 656*, 130288–130294. https://doi.org/10.1016/j.colsurfa.2022.130288

Gu, R., Li, C., Shi, X., & Xiao, H. (2022). Naturally occurring protein/polysaccharide hybrid nanoparticles for stabilizing oil-in-water Pickering emulsions and the formation mechanism. *Food Chemistry, 395*, 133641–133651. https://doi.org/10.1016/j.foodchem.2022.133641

Gu, X., Du, L., & Meng, Z. (2023). Comparative study of natural wax-based W/O emulsion gels: Microstructure and macroscopic properties. *Food Research International, 165*, 112509–112519. https://doi.org/10.1016/j.foodres.2023.112509

Gülseren, I., & Corredig, M. (2014). Interactions between polyglycerol polyricinoleate (PGPR) and pectins at the oil-water interface and their influence on the stability of water-in-oil emulsions. *Food Hydrocolloids, 34*, 154–160. https://doi.org/10.1016/j.foodhyd.2012.11.015

Guo, Y., Lin, K., Wang, Y., Dong, P., Du, P., Cao, J., Cheng, Y., Cheng, F., Yun, S., & Feng, C. (2024). Investigation on the interfacial and emulsion stabilized behavior of dextran/ferritin/resveratrol composite nanoparticles. *International Journal of Biological Macromolecules, 283*, 137533–137548. https://doi.org/10.1016/j.ijbiomac.2024.137533

Hei, X., Li, S., Liu, Z., Wu, C., Ma, X., Jiao, B., Hu, H., Zhu, J., Adhikari, B., Wang, Q., & Shi, A. (2024). Characteristics of Pickering emulsions stabilized by microgel particles of five different plant proteins and their application. *Food Chemistry, 449*, 139187–139198. https://doi.org/10.1016/j.foodchem.2024.139187

Hierro, J. N.d., Herrera, T., Fornari, T., Reglero, G., & Martin, D. (2018). The gastrointestinal behavior of saponins and its significance for their bioavailability and bioactivities. *Journal of Functional Foods, 40*, 484–497. https://doi.org/10.1016/j.jff.2017.11.032

Karaosmanoglu, S., Zhou, M., Shi, B., Zhang, X., Williams, G. R., & Chen, X. (2021). Carrier-free nanodrugs for safe and effective cancer treatment. *Journal of Controlled Release, 329*, 805–832. https://doi.org/10.1016/j.jconrel.2020.10.014

Karimi, A., Askari, G., Yarmand, M. S., Salami, M., & Djomeh, Z. E. (2020). Development, modification and characterization of ursolic acid-loaded gelatin nanoparticles through electrospraying technique. *Food and Bioproducts Processing, 124*, 329–341. https://doi.org/10.1016/j.fbp.2020.08.018

Li, B., Li, H., Su, S., Shi, M., Qin, S., & Zeng, C. (2024). Enhanced bioaccessibility of interfacial delivered oleanolic acid through self-constructed Pickering emulsion: Effects of oil types. *Food Research International, 191*, 114708–114718. https://doi.org/10.1016/j.foodres.2024.114708

Li, B., Li, Z., Li, C., Huang, X., Yu, J., zhang, Q., … Zeng, C. (2025). An effective strategy to improve the bioaccessibility of oleanolic acid in self-constructed water-in-oil emulsions: Oil phase gelation based on octacosanol. *LWT, 227*, 118041–118050. https://doi.org/10.1016/j.lwt.2025.118041

Li, Y., Wang, J., Li, L., Song, W., Li, M., Hua, X., … Xue, Z. (2023). Natural products of pentacyclic triterpenoids: From discovery to heterologous biosynthesis. *Natural Product Reports, 40*, 1303–1353. https://doi.org/10.1039/D3TC02191B

Liang, W., Deng, F., Wang, Y., Yue, W., Hu, D., Rong, J., Liu, R., Xiong, S., & Hu, Y. (2024). Interfacial behavior and micro-rheological performance of Pickering emulsions co-stabilized by β-cyclodextrin and xanthan gum. *Food Hydrocolloids, 149*, 109611–109627. https://doi.org/10.1016/j.foodhyd.2023.109611

Liu, J., Wu, Q., Lu, Y., & Pi, J. (2008). New insights into generalized hepatoprotective effects of oleanolic acid: Key roles of metallothionein and Nrf2 induction. *Biochemical Pharmacology, 76*, 922–928. https://doi.org/10.1016/j.bcp.2008.07.021

Liu, S., Liu, H., Zhang, L., Ma, C., & El-Aty, A. M. A. (2024). Edible pentacyclic triterpenes: A review of their sources, bioactivities, bioavailability, self-assembly

behavior, and emerging applications as functional delivery vehicles. *Critical Reviews in Food Science and Nutrition, 64*, 5203–5219. https://doi.org/10.1080/10408398.2022.2153238

Liu, S., Liu, Y., Li, Q., Song, Y., Zhang, L., Peng, F., & Ma, C. (2024). Oleanolic acid nanoparticles-stabilized W/O Pickering emulsions: Fabrication, characterization, and delivery application. *Food Chemistry, 444*, 138598–138608. https://doi.org/10.1016/j.foodchem.2024.138598

Liu, Y., Xia, H., Guo, S., Li, P., Qin, S., Shi, M., & Zeng, C. (2023). Effect and mechanism of edible oil co-digestion on the bioaccessibility and bioavailability of ursolic acid. *Food Chemistry, 423*, 136220–136231. https://doi.org/10.1016/j.foodchem.2023.136220

Liu, Y., Xia, H., Guo, S., Lu, X., & Zeng, C. (2022). Development and characterization of a novel naturally occurring pentacyclic triterpene self-stabilized Pickering emulsion. *Colloids and Surfaces A: Physicochemical and Engineering Aspects, 634*, 127908–127918. https://doi.org/10.1016/j.colsurfa.2021.127908

Liu, S., Zhang, J., Fu, R., Feng, H., Chu, Y., Huang, D., … El-Aty, A. M. A. (2022). Improved stability and aqueous solubility of β-carotene *via* encapsulation in self-assembled bioactive oleanolic acid nanoparticles. *Food Chemistry, 373*, 131498–131506. https://doi.org/10.1016/j.foodchem.2021.131498

Montesano, D., Rocchetti, G., Putnik, P., & Lucini, L. (2018). Bioactive profile of pumpkin: An overview on terpenoids and their health-promoting properties. *Current Opinion in Food Science, 22*, 81–87. https://doi.org/10.1016/j.cofs.2018.02.003

Mu, M., Zhou, W., Arcot, Y., Cisneros-Zevallos, L., & Akbulut, M. (2024). Edible superhydrophobic coating derived from triterpenoid maslinic acid for bacterial antifouling and enhanced fresh produce food safety. *Food Packaging and Shelf Life, 43*, 101290–101299. https://doi.org/10.1016/j.fpsl.2024.101290

Pan, Y., Xu, X., Zhao, W., Tian, F., Zhao, Y., Zhang, T., Yang, H., Han, J., & Liu, W. (2025). Chitosan-polygalacturonic acid-double-layered liposomes for oleanolic acid delivery: *In vitro* semi-dynamic digestion, improved cell uptake and liver protection. *International Journal of Biological Macromolecules, 308*, 142534–142546. https://doi.org/10.1016/j.ijbiomac.2025.142534

Qin, X., Yu, J., Wang, Q., Zhang, H., Chen, H., Hu, Z., … Liu, G. (2022). Preparation of camellia oil Pickering emulsion stabilized by glycated whey protein isolate and chitooligosaccharide: Effect on interfacial behavior and emulsion stability. *LWT, 153*, 112515–112522. https://doi.org/10.1016/j.lwt.2021.112515

Si, L., Meng, K., Tian, Z., Sun, J., Li, H., Zhang, Z., Soloveva, V., Li, H., Fu, G., Xia, Q., Xiao, S., Zhang, L., & Zhou, D. (2018). Triterpenoids manipulate a broad range of virus-host fusion via wrapping the HR2 domain prevalent in viral envelopes. *Science Advances, 4*, 8408–8453. https://doi.org/10.1126/sciadv.aau8408

Sohag, A. A. M., Hossain, M. T., Rahaman, M. A., Rahman, P., Hasan, M. S., Das, R. C., … Hannan, M. A. (2022). Molecular pharmacology and therapeutic advances of the pentacyclic triterpene lupeol. *Phytomedicine, 99*, 154012–154031. https://doi.org/10.1016/j.phymed.2022.154012

Tang, Z., Li, Y., Tang, Y., Ma, X., & Tang, Z. (2022). Anticancer activity of oleanolic acid and its derivatives: Recent advances in evidence, target profiling and mechanisms of action. *Biomedicine & Pharmacotherapy, 145*, 112397–112418. https://doi.org/10.1016/j.biopha.2021.112397

Thakur, N., Raigond, P., Singh, Y., Mishra, T., Singh, B., Lal, M. K., & Dutt, S. (2020). Recent updates on bioaccessibility of phytonutrients. *Trends in Food Science & Technology, 97*, 366–380. https://doi.org/10.1016/j.tifs.2020.01.019

Ting, Y., Jiang, Y., Zhao, S., Li, C. C., Nibber, T., & Huang, Q. (2018). Self-nanoemulsifying system (SNES) enhanced oral bioavailability of boswellic acids. *Journal of Functional Foods, 40*, 520–526. https://doi.org/10.1016/j.jff.2017.11.043

Wang, J., Zhao, H., Zhi, K., & Yang, X. (2020). Exploration of the natural active small-molecule drug-loading process and highly efficient synergistic antitumor efficacy. *ACS Applied Materials & Interfaces, 12*, 6827–6839. https://doi.org/10.1021/acsami.9b18443

Wang, Q., Espert, M., Hern'andez, M. J., Salvador, A., & Sanz, T. (2024). Effect of cellulose ether emulsion and oleogel as healthy fat alternatives in cream cheese. Linear and nonlinear rheology, texture and sensory properties. *Food Hydrocolloids, 150*, 109740–109748. https://doi.org/10.1016/j.foodhyd.2024.109740

Wang, X., Ye, X., Liu, R., Chen, H., Bai, H., Liang, X., … Hai, C. (2010). Antioxidant activities of oleanolic acid *in vitro*: Possible role of Nrf2 and MAP kinases. *Chemico-Biological Interactions, 184*, 328–337. https://doi.org/10.1016/j.cbi.2010.01.034

Yan, Y., Liu, Y., Zeng, C., & Xia, H. (2023). Effect of digestion on ursolic acid self-stabilized water-in-oil emulsion: Role of bile salts. *Foods, 12*, 3657–3663. https://doi.org/10.3390/foods12193657

Zeng, C., Wang, Y., Liu, Y., Su, S., Lu, Y., Qin, S., & Shi, M. (2024). Self-constructed water-in-oil Pickering emulsions as a tool for increasing bioaccessibility of betulin. *Food Chemistry: X, 21*, 101056–101064. https://doi.org/10.1016/j.fochx.2023.101056

Zhou, J., Wei, X., Chen, F., Li, C., Yang, J., Ma, J., Bao, X., Zhang, D., & Zhang, D. (2017). Anti-inflammatory pentacyclic triterpenes from the stems of *Euonymus carnosus*. *Fitoterapia, 118*, 21–26. https://doi.org/10.1016/j.fitote.2017.01.015

Zhou, L., Jiang, J., Feng, F., Wang, J., Cai, J., Xing, L., Zhou, G., & Zhang, W. (2023). Effects of carboxymethyl cellulose on the emulsifying, gel and digestive properties of myofibrillar protein-soybean oil emulsion. *Carbohydrate Polymers, 309*, 120679–120688. https://doi.org/10.1016/j.carbpol.2023.120679